Control of Flat Band Voltage by Partial Incorporation of La_2O_3 or Sc_2O_3 into HfO_2 in Metal/HfO_2/SiO_2/Si MOS Capacitors

M. Adachi[1], K. Okamoto[1], K. Kakushima[2], P. Ahmet [1],
K. Tsutsui[2], N. Sugii[2], T. Hattori[1] and H. Iwai[1]
[1]Frontier Collaborative Research Center, Tokyo Institute of Technology,
4259-S2-20, Nagatsuta, Midori-ku, Yokohama 226-8502, Japan
[2]Interdisciplinary Graduate School of Science and Engineering, Tokyo Institute of Technology, 4259-S2-20 Nagatsuta, Midori-ku, Yokohama 226-8502, Japan

Abstract

High-k/SiO_2 interfacial properties are most critical factors determining the high-k gate MOSFET characteristics. We fabricated MOS capacitors of metal/HfO_2/SiO_2/Si structures in which were contained in the HfO_2 layer. Flat-band voltage (V_{FB}) shifts were measured by changing composition in metal/HfO_2/$(HfO_2)_{1-x}(La_2O_3)_x$/SiO_2/Si and metal/HfO_2/$(HfO_2)_{1-x}(Sc_2O_3)_x$/SiO_2/Si structures. It was found that V_{FB} shift arises mainly from high-k/SiO_2 interface rather than metal/high-k interface. V_{FB} could be effectively controlled by incorporating La_2O_3 or Sc_2O_3 near the high-k/SiO_2 interface.

Introduction

Combination of metal and high-k dielectrics is necessary in order to achieve smaller EOT for eliminating the poly-Si gate depletion effect without excess leakage current. HfO_2 based materials have been the promising candidates for next generation gate dielectric thanks to its high temperature endurance and relatively high permittivity. One of the issues of HfO_2 based oxides is the difficulty in reducing the threshold voltage (*Vth*) as relatively high *Vth* were obtained with HfO_2 based oxides whatever the electrode material is. On the other hand, it has been reported that La_2O_3 and Sc_2O_3 produce negative shift in V_{FB} with respect to HfO_2 reference [1]. However, the detailed mechanism is not clarified yet. In this paper, first we extract the effective work function (*EWF*) of tungsten gate metal on high-k dielectrics, and then investigated the effect of La_2O_3 or Sc_2O_3 incorporation into a HfO_2 layer in a metal/HfO_2/SiO_2/Si MOS capacitor.

Experimental

Si(100) substrates with 200 nm-thick field SiO_2 in which diode holes were opened (1-10 ohm-cm) were cleaned in a mixed solution of H_2SO_4 and H_2O_2, followed by dipping in diluted HF. The substrates were then thermally oxidized to grow 3.5-nm-thick SiO_2 film. High-k dielectrics were deposited on these substrates by e-beam evaporation with O_2 partial pressure of 1×10^{-4} Pa. Tungsten (W) gate electrode was *in-situ* deposited by RF sputtering. The W film was lithographically patterned and etched by reactive ion etching (RIE) using SF_6 chemistry to form gate electrodes for MOS capacitors. Annealing in forming gas (3 %-H_2+97 %-N_2) was performed at 420 ^{o}C for 30 min. Finally, aluminum (Al) was thermally evaporated on backside of the wafers for bottom electrode. Capacitance-voltage (*C-V*) characteristics of the fabricated MOS capacitors were measured at 100 kHz using Agilent 4284A precision LCR meter, from which V_{FB} and EOT were calculated using NCSU CVC program.

The dielectrics studied here are La_2O_3, HfO_2 and Sc_2O_3. To evaluate the main reason of V_{FB} shift, laminated dielectric stacks of HfO_2/La_2O_3 were fabricated. Moreover, mixed dielectrics of HfO_2-La_2O_3 and HfO_2-Sc_2O_3 with HfO_2 atop were also fabricated by co-evaporation of the two oxides.

Results and Discussions

Effective Work Function *(EWF)* Extraction

A schematic model of the charge locations in a metal/SiO_2/Si structure and metal/high-k/SiO_2/Si structure are illustrated in Fig.1. As the thickness of the dielectric layer is small, the bulk charges of each oxide can be neglected. Indeed, the results shown in Fig. 2 revealed a linear relationship between V_{FB} and the EOT, thus, it is reasonable to assume low charge concentration inside the SiO_2 and the high-k layer. Under the assumption, the effective work function (*EWF)* of metal on a SiO_2 can be derived from the relation of V_{FB} and EOT using the following equation,

$$V_{FB} = -\left(\frac{Q_{SiO2/Si}}{\varepsilon_0 \varepsilon_{ox}}\right) \cdot EOT + \frac{\varphi_{ms}}{q} + q\Delta_{SiO2/Metal}, \qquad (1)$$

where $Q_{SiO2/Si}$ is the fixed charge at the SiO_2/Si interface, φ_{ms} is the work function difference of gate metal and semiconductor and $\Delta_{SiO2/Metal}$ is the dipole at metal/oxide interface. The *EWF* of gate metal, defined as $\frac{\varphi_{ms}}{q} + q\Delta_{SiO2/Metal}$, can be extracted by the y-intercept from the V_{FB}-EOT slope. When interfacial SiO_2 layer (IL) is inserted between high-k dielectric and Si substrate, the Eq.(1) can be modified using total EOT as shown in eq.(2),

$$V_{FB} = -\left(\frac{Q_{high-k/IL} + Q_{SiO2/Si}}{\varepsilon_0 \varepsilon_{ox}}\right) \cdot EOT + \frac{Q_{SiO2/high-k}}{\varepsilon_0 \varepsilon_{ox}} \cdot EOT_{IL} + \frac{\varphi_{ms}}{q} + q\Delta_{Metal/high-k}. \qquad (2)$$

Here, $Q_{high-k/IL}$, $\Delta_{high-k/Metal}$ and EOT_{IL} are the fixed charge at high-k/IL interface, the dipole at high-k/metal interface and the EOT of IL, respectively. Eventually, the *EWF* of metal on high-k/SiO_2 stack can be expressed as follows,

$$EWF_{(high-k)} = EWF_{(SiO2)} + (q\Delta_{high-k/Metal} - q\Delta_{SiO2/Metal}). \qquad (3)$$

Figure 2 shows the typical *C-V* curves of La_2O_3/IL, HfO_2/IL and Sc_2O_3/IL capacitors. The difference between V_{FB}(HfO_2/IL) and V_{FB}(La_2O_3/IL) is about 0.48 V, whereas difference between V_{FB}(HfO_2/SiO_2) and V_{FB}(Sc_2O_3/SiO_2) is 0.15 V. Figure 3 shows the result of V_{FB} of La_2O_3/IL, HfO_2/IL and Sc_2O_3/IL capacitors with different high-k thicknesses. Capacitors with SiO_2 with different thickness are also shown to derive $Q_{SiO2/Si}$. Using the equations (1)-(3), *EWF* of W on SiO_2, HfO_2, La_2O_3 and Sc_2O_3 can be calculated and summarized in Table.1. The smallest *EWF* of 4.46 eV was obtained with La_2O_3, whereas relatively large value was obtained with HfO_2. These results suggest high

V_{th} in nMOSFET when HfO_2 is used as gate dielectrics. In the next subsection, the origin of V_{FB} is examined in detail.

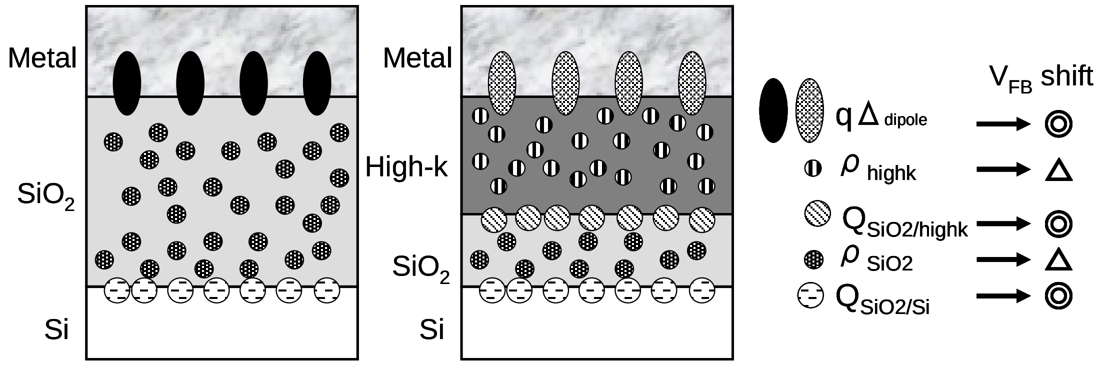

Fig.1 Schematic model of the charge locations used in the extraction of fixed charge.

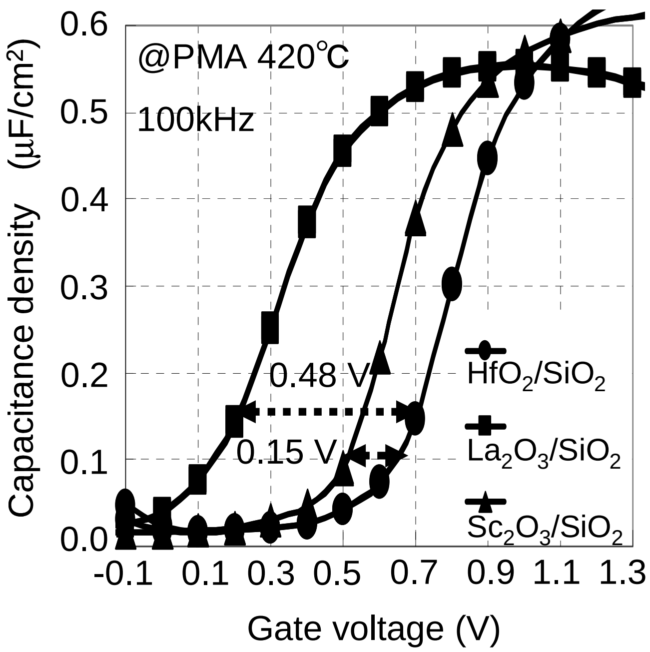

Fig.2 *C-V* characteristics of MOS capacitors with single layered high-k dielectric (HfO_2, La_2O_3, Sc_2O_3)

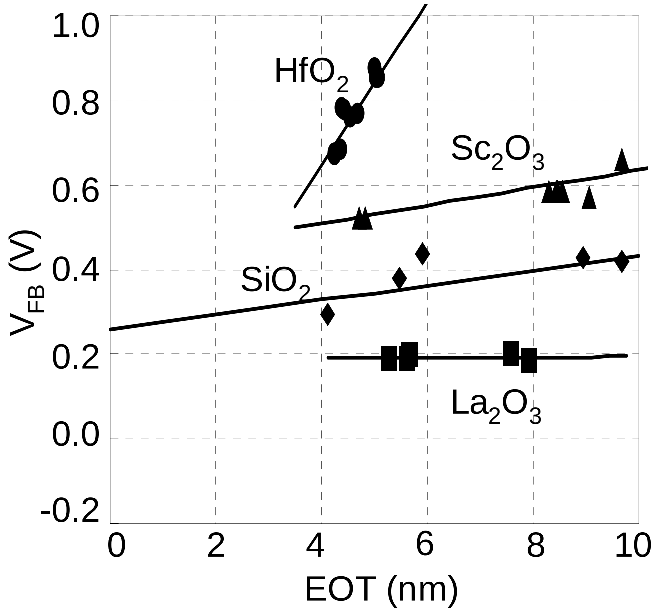

Fig.3 V_{FB}-EOT plot obtained from the analysis of *C*-*V* curves.

Table 1. Effective work function of W gate electrode on various gate dielectric (SiO_2, La_2O_3, HfO_2, La_2O_3)

Gate Oxide	SiO_2	La_2O_3	HfO_2	Sc_2O_3
EWF (eV)	4.59	4.46	4.80	4.75

C-V Characteristics of HfO_2/La_2O_3 Stack Structure

In order to investigate the V_{FB} shift on stacked dielectrics, double layer stacked films were fabricated, as shown in Fig. 4. Capacitors with single layer of HfO_2 or La_2O_3 are also fabricated as references. The total thickness of the high-k film was designed to have 5 nm. Figure 5 shows the C-V characteristics of $W/HfO_2/La_2O_3$/IL stacked MOS capacitors. The C-V curves of the stacked capacitors showed negative V_{FB}, which are close to that of the single La_2O_3 layer reference. From these results, it is clear that the V_{FB} shift is determined by the high-k material in contact to SiO_2 IL. It is known that positive charges or dipole at the interface could attribute to negative shift in V_{FB}, however, either or both effects on these results are not clarified yet. Nonetheless, it is expected that by changing the composition of high-k at the high-k/IL interface might allow precise V_{FB} control.

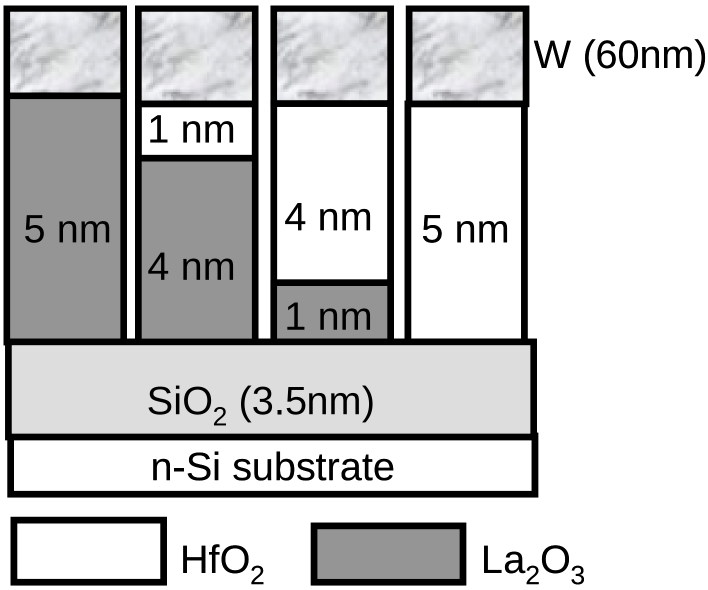

Fig.4 Schematic illustration of fabricated MOS capacitors with stack of HfO_2 and La_2O_3. Capacitors with single HfO_2 or La_2O_3 layer are fabricated as references.

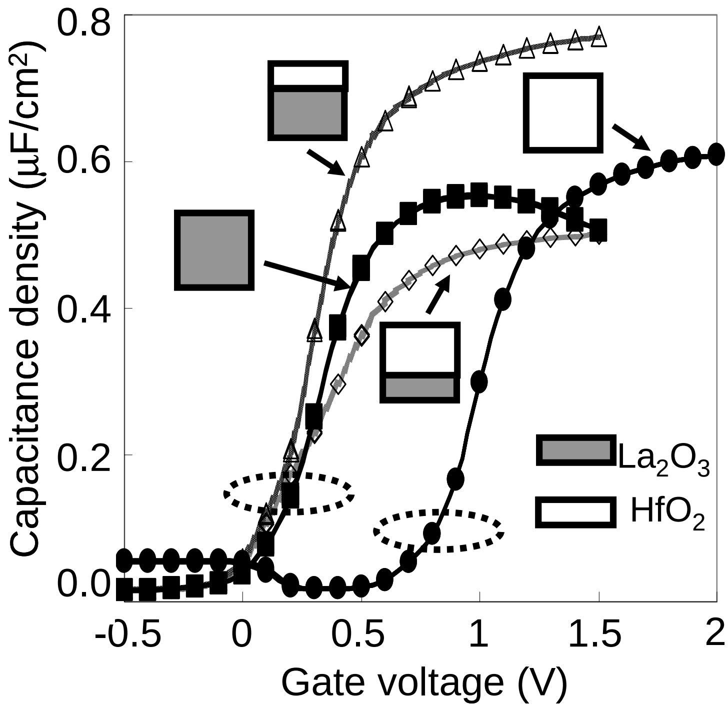

Fig.5 *C*-*V* curves for W/HfO_2/La_2O_3/SiO_2 stacked MOS capacitors.

<u>V_{FB} Shift Dependence on La_2O_3 Incorporation at High-k/SiO_2 Interface</u>

In this subsection, the V_{FB} shift depending on the amount of La_2O_3 at the high-k/SiO_2 interface is investigated. From the result that even 1 nm of La_2O_3 at high-k/SiO_2 interface can negatively shift the V_{FB}, the amount of the incorporated La_2O_3 to realize controllability of V_{FB} should be less than 1 nm. To obtain precise controllability of amount of La_2O_3 during the deposition process, we employed co-evaporation of HfO_2 and La_2O_3 with different concentration, those are 20, 50 and 80 %. The thickness of the mixed high-k layers was set to 1 nm. HfO_2 with 5 nm thickness was capped on the mixed high-k. The schematic illustrations of the fabricated capacitors are shown in Fig. 6. The *C*-*V* characteristics of the mixed high-k stack capacitors together with those of the references with La_2O_3 and HfO_2 capacitors are shown in Fig. 7. With the La_2O_3 concentration of 80%, the V_{FB} of *C*-*V* curves showed almost identical value for the La_2O_3 reference, where that of 20 % showed in between of those of HfO_2 and La_2O_3 references. With 50 % of La_2O_3 incorporation, the V_{FB} was slightly positive to the La_2O_3 reference. Also from these results, it is noted that the *EWF* of the gate metal is mainly dominated by the high-k/IL interface, not at the Metal/high-k interface. By plotting the V_{FB} on La_2O_3 concentration, as is shown in Fig. 8, we obtain a monotonic relation between concentration and V_{FB}. It can be concluded that V_{FB} can be effectively controlled by changing the concentration of the mixed high-k at the high-k/IL interface.

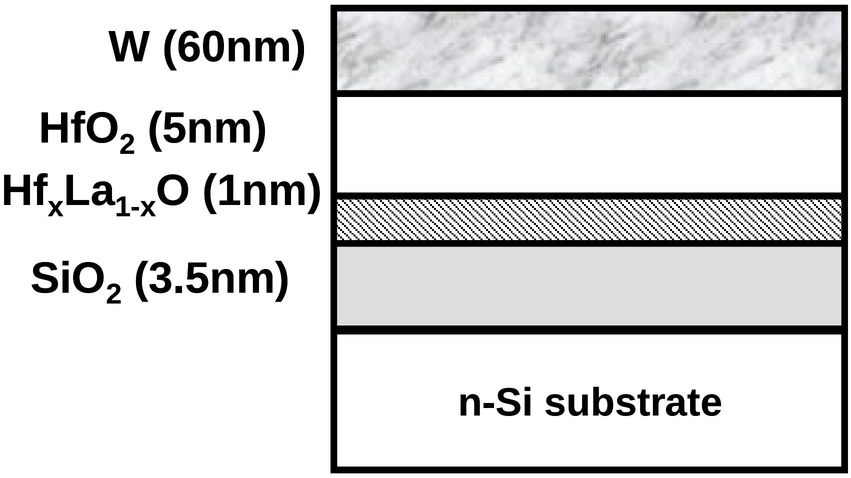

Fig.6 Schematic illustration of fabricated MOS capacitor incorporating La_2O_3 into HfO_2/SiO_2 interface

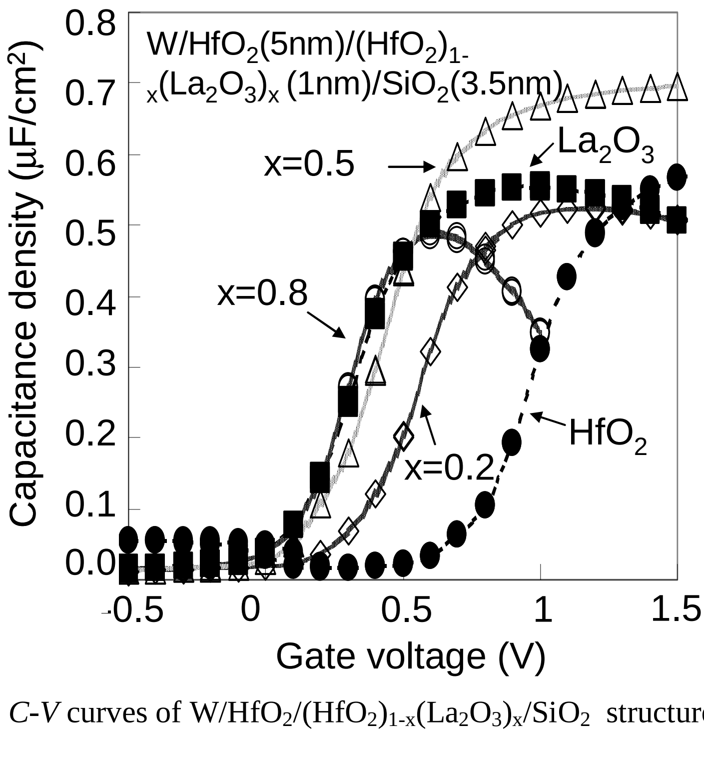

Fig.7 *C*-*V* curves of $W/HfO_2/(HfO_2)_{1-x}(La_2O_3)_x/SiO_2$ structure

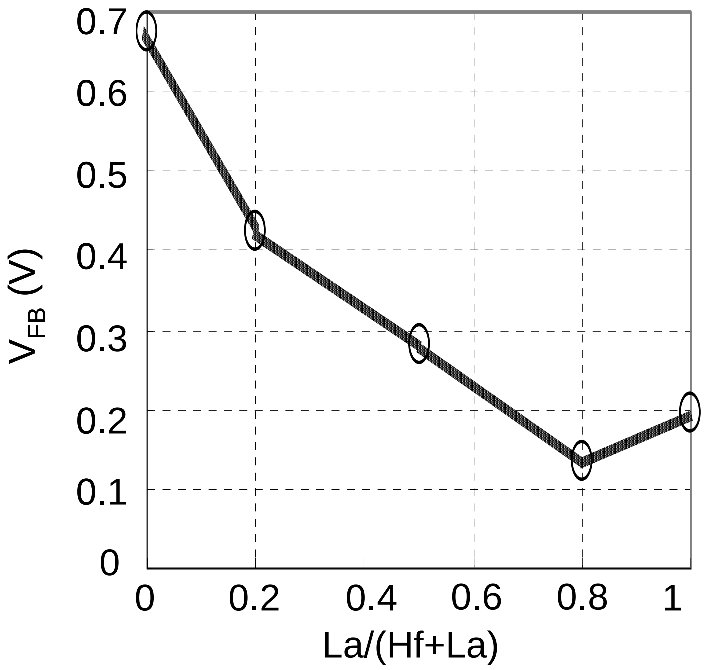

Fig.8 V_{FB} shift depending on concentration of incorporation La at HfO_2/SiO_2

<u>V_{FB} Controlled by Sc_2O_3 Incorporation into HfO_2</u>

The same experiments were carried out using Sc_2O_3 and HfO_2. In this case, the thickness of Sc_2O_3-HfO_2 mixed high-k and HfO_2 capping layer were set to 5 nm and 0.5 nm, respectively. The structure is depicted in Fig. 9. The concentrations of Sc_2O_3 were set to 33, 50 and 67%. Figure 10 shows the *C*-*V* curves of the Sc_2O_3 incorporated HfO_2 capacitors. Also Sc_2O_3 and HfO_2 references are shown. Negative shifts of V_{FB} with increase in the concentration of Sc_2O_3 were obtained. The relation between the concentration and V_{FB} is shown in Fig. 11. From this figure, the V_{FB} control range of 0.15 V was achieved using Sc_2O_3 incorporation into HfO_2. This value is smaller than that of La_2O_3, which can be expected from Sc_2O_3 single layer capacitor. Therefore, Sc_2O_3 and La_2O_3 incorporation technique is useful as fine and coarse tuning of V_{FB}, respectively.

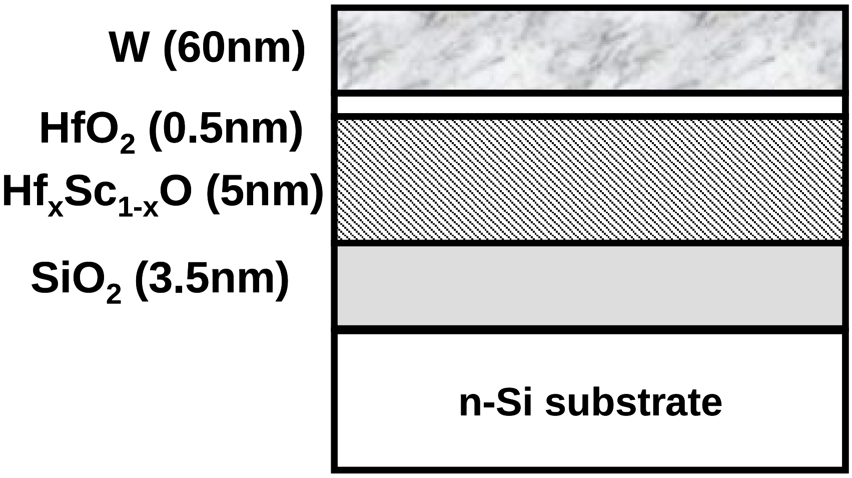

Fig.9 Schematic illustration of fabricated MOS capacitors incorporating Sc_2O_3 into HfO_2/SiO_2 interface

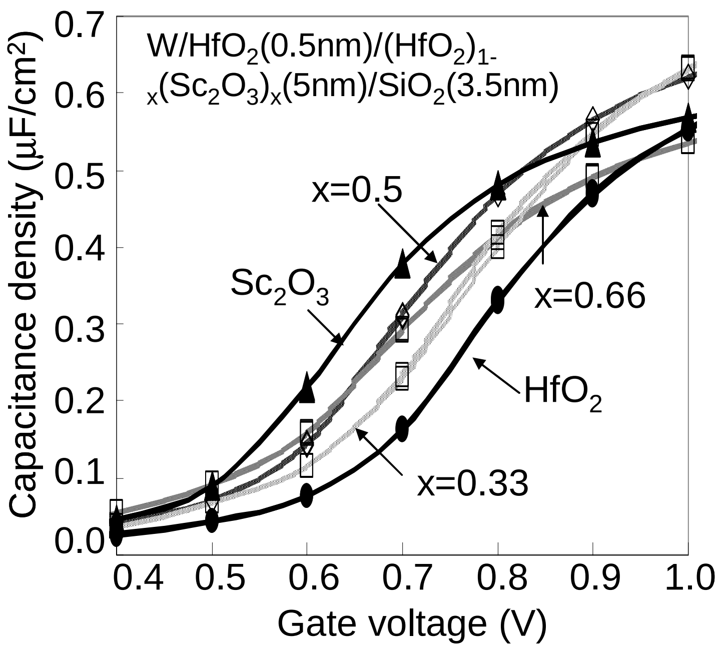

Fig.10 *C-V* curves of $W/HfO_2/(HfO_2)_{1-x}(Sc_2O_3)_x/SiO_2$ structures.

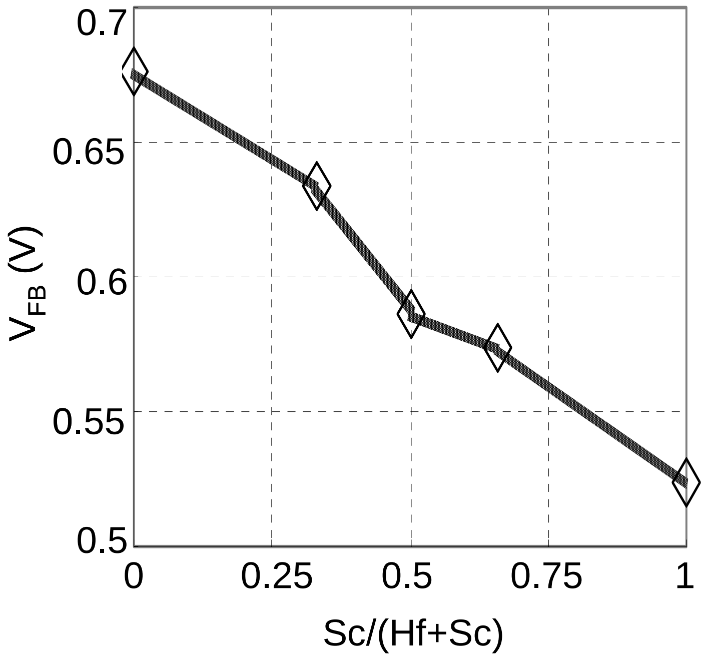

Fig.11 V_{FB} shift depending on incorporation of Sc at HfO_2/SiO_2 interface

Conclusions

The V_{FB} shift was found to be dominated by the high-k/SiO_2 interface property. The most considerable causation is an existence of the dipole at the high-k/SiO_2 interface. We observed the V_{FB} shift for the MOS capacitors using $(HfO_2)_{1-x}(La_2O_3)_x/SiO_2$ or $(HfO_2)_{1-x}(Sc_2O_3)_x/SiO_2$ as gate dielectrics. The V_{FB} is dependent on concentration of La_2O_3 or Sc_2O_3, and the large concentration results in large negative V_{FB} shift up to the V_{FB} obtained for the capacitors using La_2O_3/SiO_2 or Sc_2O_3/SiO_2. Coarse and fine tuning of V_{FB} for HfO_2 gate dielectrics were successfully observed by La_2O_3 and Sc_2O_3 incorporation, respectively. V_{FB} of MOS capacitors using high-k dielectrics could be controlled by the incorporation of La_2O_3 or Sc_2O_3 at the HfO_2/SiO_2 interface.

Acknowledgments

This work is partially supported by New Energy and Industrial Technology Develop Organization (NEDO).

References

[1] Y. Yamamoto, et al., Ext. Abst. of SSDM p.212, (2006)

[2] Vidya S. Kaushik et al., IEEE Transaction on Electron Devices Vol 53, No10, (2006)

[3] M. Kadoshima, et al., Symposium on VLSI Technology Digest of Technical Papers, p.226, (2006)

[4] Rashmi Jha et al., IEEE Electron Device Letters, Vol 25, No6, June (2004)

[5] "NCSU CVC Analysis, Version 5.0", (North Carolina State University, 2000).